7. ANKARA INTERNATIONAL AEROSPACE CONFERENCE
11-13 September 2013 - METU, Ankara TURKEY

AIAC-2013-053

EFFECT OF BLADE-TIP GEOMETRY ON TURBINE LOSSES AND FILM COOLING EFFECTIVENES

Ahmed M. Elsayed [1]
Institute of Aviation Engineering and Technology
Giza, Egypt

Farouk M.Owis[2]
Cairo University
Giza, Egypt

Mohamed.M.Abdelrahman [3]
Cairo University
Giza, Egypt

ABSTRACT

The tip leakage flow across the turbine blade reduces its aerodynamic performance and causes blade-tip overheating due to this high speed flow and the existence of a thin boundary layer. Different blade-tip configurations are used in turbines including flat tip, single squealer and double squealer. The effect of these configurations on the turbine losses is investigated numerically in the current study using the CFDRC-ACE package. In addition, a parameteric study on the tip film cooling is performed to select the optimum parameters such as blowing ratio, streamwise angle and film cooling hole. Unstructured finite volume technique is used to solve the steady, three-dimensional and compressible Navier-Stokes equations. The total pressure loss coefficient and the cooling effectiveness are computed for GE-E[3] turbine blade of different tip clearances and different depths for the squealer cavity. The results indicate that the single squealer tip shape with cooling hole located at tip pressure side has minimum tip flow losses and maximum cooling effectiveness. The film cooling effectiveness on the blade tip is enhanced by decreasing the streamwise angle for high blowing ratio.

INTRODUCTION

The sources of inefficiency in turbines are due to a number of unavoidable processes. These are generally categorized as profile loss and end wall loss, secondary flow losses and tip leakage loss. Each of these processes generates entropy. The tip gap is an unavoidable clearance between an unshrouded rotor blade tip and the stationary outer casing or end wall. The size of the tip clearance is dependent on the engine operating conditions. To avoid rubbing, a minimum clearance of 1-3.5% of the blade height is needed. The losses associated with tip clearance are a slightly more complicated process. Entropy is generated by viscous shearing on the tip surfaces, mixing of separated flow within the gap as well as by the subsequent mixing of the leakage flow into the passage flow between the rotor blades and also downstream of the rotor. In a reaction turbine, the pressure differential across the blade surfaces causes fluid to leak through the gap with the creation of entropy. This fluid then enters the blade passage flow at a highly sheared angle and forms a vortex structure in the blade suction corner near the tip.

One of the most critical areas, from a thermal point of view, is the tip region of the un-shrouded rotor blades. Tip regions are generally cooled using rotor internal air ejected in the flow path through a series of small holes located in the tip surfaces. The ejected air must cover all the surfaces in order to create a cold film between the hot gas and the metal. As the tip-region is characterized by a very complex 3D flow field, it is difficult to optimize the cooling system using the standard design methodologies. In addition, the blade tip configuration is designed such that the tip leakage from the pressure side to the suction side of the blade is minimized. In the current study, the configuration of the tip is investigated numerically to select the tip parameters for minimum tip losses and optimum film cooling.

Several researchers investigated the blade tip clearance and its effects on the turbine efficiency and turbine cooling [Azad, 2000; Heyes, 1992; Bunker, 2000]. A numerical heat transfer investigation of a turbine tip section with a mean camber-line strip is investigated [Ameri, 2001] for a large power-

[1] Ass. Teacher. İn Aerospace Department, Email: ac_eng_sayed@yahoo.com
[2] Ass. Prof. İn Aerospace Department, Email: fowis@eng.cu.edu.eg
[3] Prof. İn Aerospace Department, Email: Dr_madbouli@hotmail.com

generating turbine. A radiused-edge tip and a sharp-edge tip are investigated with a mean camber-line strip on the tip surface. The favorable conditions created by using a sharp edge tip are shown. Effects of a squealer tip covering the complete perimeter on rotor heat transfer and efficiency is presented in a numerical study by Ameri, Steinthorsson and Rigby [Ameri, 1997].

A comprehensive investigation of the effect of squealer geometry on gas turbine blade tip heat transfer is presented by Azad, Han, Bunker and Lee [Azad, 2001]. In addition to tip heat transfer results in a five bladed linear cascade, stationary shroud wall static pressures are used for leakage flow field interpretation.

Ameri and Bunker [Ameri and Bunker, 2000] performed a computational study to investigate the detailed heat transfer distributions on blade tip surfaces for a large power generation turbine and the results are compared with the experimental data of Bunker et al. [Ameri and Bunker, 2000]. The flow and heat transfer of on a blade tip with a mean-camber line strip are computed by Ameri et al. [Ameri, 2001]. Yang et al. [Yang and Bunker, 2002] studied numerically the flow and heat transfer around the $\mathrm{GE\text{-}E^3}$ blade with a flat tip and a squealer tip for different turbulent models. The predicted heat transfer coefficients are in reasonable agreement with the experimental results of Azad et al. [Azad, 2000].

More recently, [Kwak and Han, 2003; Christophel et al., 2005] used thermal imaging techniques to measure detailed film cooling effectiveness contours on the tip with holes on the pressure side of the tip region. In general, previous studies show that a higher blowing ratio with small tip clearance results in better film cooling performance. [Ahn, 2005; Mhetras, 2008] measured effectiveness using the PSP technique with holes on the pressure side of the tip region. et al. [Gao, 2009] characterized the effect of blade angle-of-attack on film cooling effectiveness using the PSP technique.

The effect of coolant mainstream blowing ratio is investigated by Rallabandi et al. [Rallabandi, 2008]. The study indicates that regardless of hole-shape and angle, film cooling effectiveness increases at low blowing ratios. However, beyond a critical blowing ratio, film cooling effectiveness declines. This result can be attributed to the phenomenon of film-cooling lift-off.

The objective of the current study is to optimize the blade tip configuration for minimum turbine losses and higher film cooling effectiveness. The effect of different tip configurations on the tip leakage losses and tip film cooling are studied numerically to determine the tip shape. The flow on the different tip shape of turbine blade with film cooling is numerically simulated using the steady, compressible Navier-Stokes equations with turbulence modeling. The computations are performed using the CFDRC package. The solver uses the three-dimensional steady compressible viscous flow field coupled with the k-ε turbulence model. An unstructured grid is used for the simulations on the turbine blade. The governing equations are discretized using the finite volume technique with second order accuracy in space. The flat and squealer tip shapes are defined by tip clearance (C) that is varied in the range of 1.5 to 3.5% of the blade span. However, the depth of the squealer cavity (D) is varied from 2.1 to 6.3% of the blade span. An array of seven cooling-hole is used for the tip film cooling. The hole geometry is defined in terms of three variables which are the streamwise angle (α), the cooling hole position to blade tip thickness ratio (L/t) and the coolant blowing ratio (M. The streamwise angle (α) is assumed to vary from 30 to 90 degree. The cooling hole position to blade tip thickness ratio (L/t) is assumed to vary from 0.2 to 0.8 while the coolant blowing ratio (M) is varied from 0.5 to 2.

NUMERICAL MODEL

Turbine Blade Numerical Simulations

The present calculations are performed for a $\mathrm{GE\text{-}E^3}$ blade. Figure 1 shows the geometry for the $\mathrm{GE\text{-}E^3}$ blade with different blade tip configurations. Different blade tip configurations of flat tip, double squealer tip and single suction side squealer tip of untwisted blade with cylindrically hub and casing surfaces are presented in Figure 1. The left side bottom of Figure 1 illustrates a schematic of the complete turbine rotor geometry. On right side bottom of Figure1, a schematic of the blade with three different cutting planes are shown. These planes are used to demonstrate the flow structures around the blade tip region.

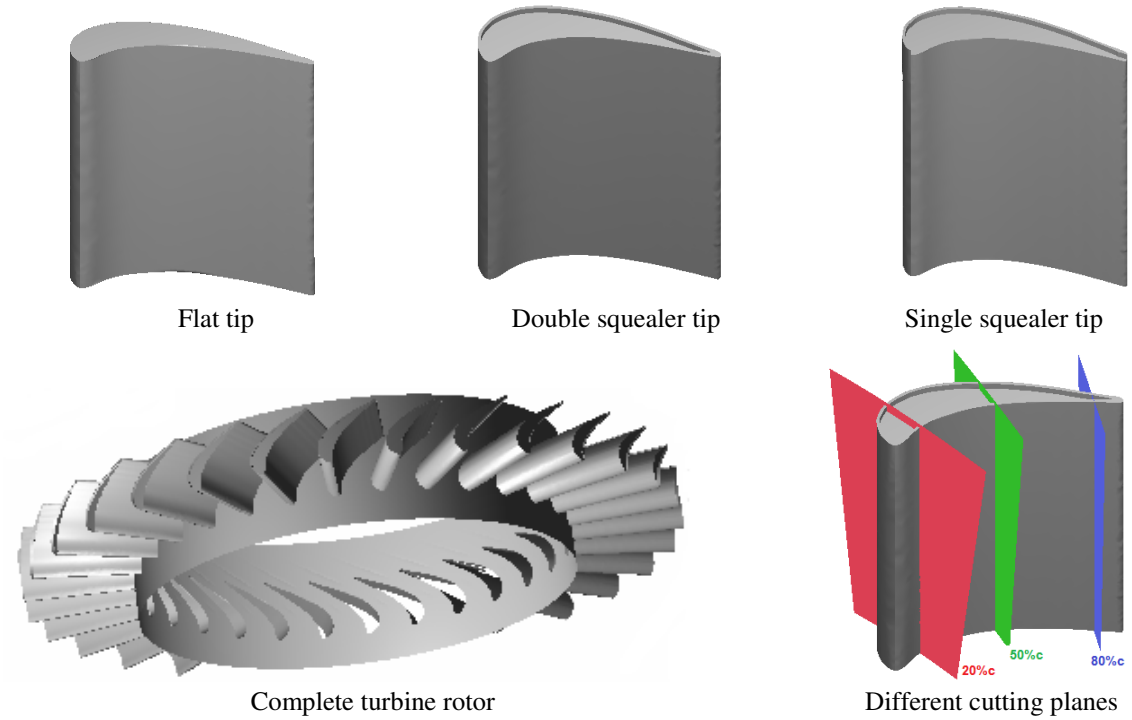

Figure 1: *Three tip configurations and schematic of the computational domain with different cross sectional planes*

Computational Model Grid

The CFD-Geom of CFDRC software is used to generate a tetrahedral-hybrid unstructured grid for one blade of complete turbine blades. A Grid function is used to adjust the grid size near wall and tip regions as shown in Figure 2. A minimum cell size of 0.2 mm is used at the high curvature area around the cooling hole with a growth rate of 1.1. A maximum cell size of 2 mm is used at the low curvature area (straight area). The growth rate factor is used to adjust the grid number between the two areas. The total number of cells used for the numerical simulations is 1.5 million cells.

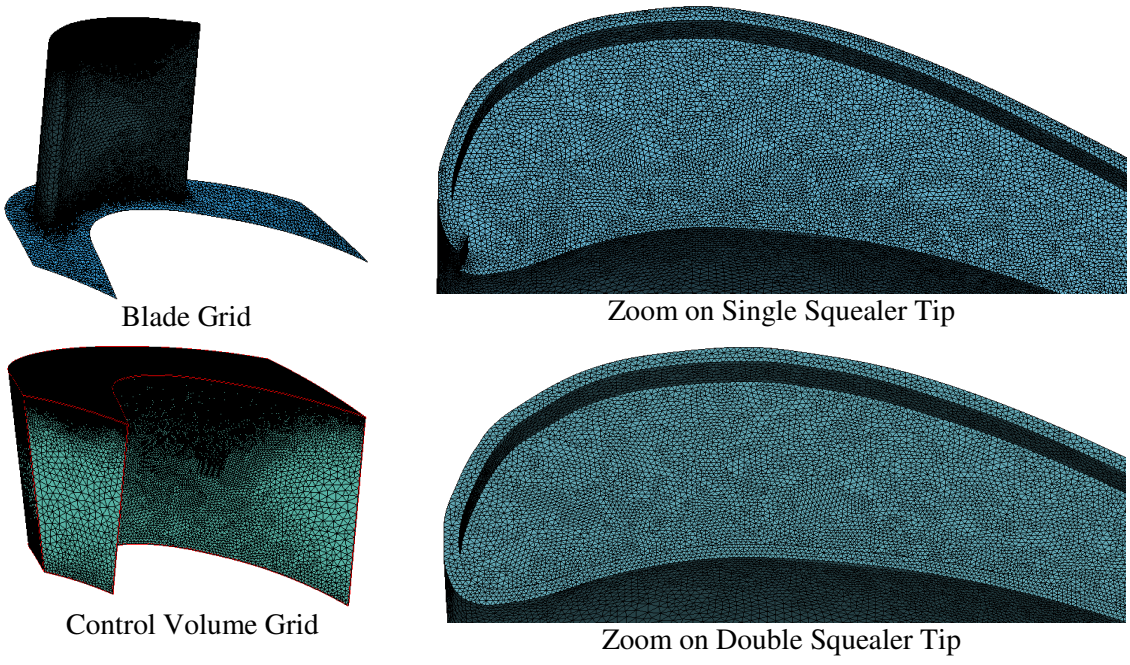

Figure 2: *Computational grid for single squealer and double squealer tips*

Cooling Hole Geometry

The selected geometry of the cooling-hole system is taken as one cooling hole array that contains seven cylindrically-round simple-angle (CYSA) holes type. The holes are assumed to be separated by an equal distance. The position of the cooling holes is changed from the tip pressure side to tip suction side by changing the variable L/t. The position of cooling hole array lies on the blade tip camber line when $\frac{L}{t}$ equals 0.5 . The cooling hole diameter (D) is selected to be 1.3 mm and the cooling fluid is injected to the mainstream at a streamwise angle (α) which is varied from 30° to 90° as shown in Figure 3.

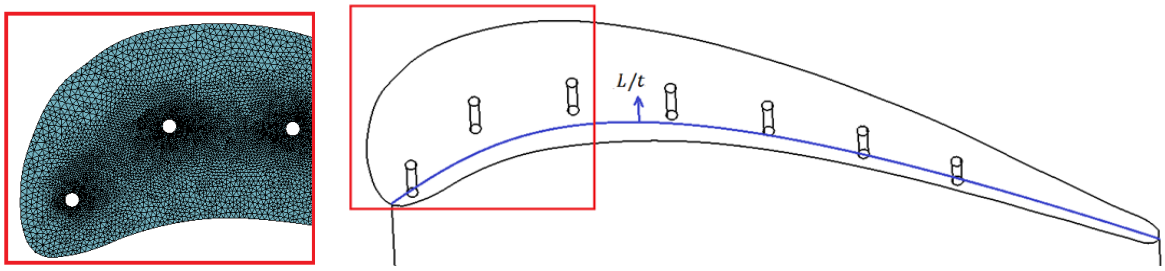

Figure 3: *Cooling-holes configuration and grid*

Boundary Conditions

The computational domain consists of a single blade with periodic conditions imposed along the boundaries in the circumferential (theta) direction. The inlet boundary is placed at one-half chord length upstream of the blade so that simple uniform inflow boundary conditions can be employed. The total inlet temperature is assumed to be 1700 K while the total pressure is taken to be 1.675 MPa. An inlet flow angle of 32 degree is used in the simulations and the turbulence intensity level is assumed to be 9.6%. The inlet flow velocity is 183 m/sec. The exit boundary is located at one chord length downstream of the blade trailing edge to provide appropriate resolution of the tip leakage flow and passage vortices. The exit static pressure is specified to be 1.03 MPa. Therefore, the inlet total pressure to the outlet static pressure ratio (PR=$P_{in,t}/P_{out}$) is 1.63. On the blade surface, the no-slip condition is specified. A rotating speed of 9,600 rpm is used in the present simulations while the shroud remains stationary, as shown in Figure 4.

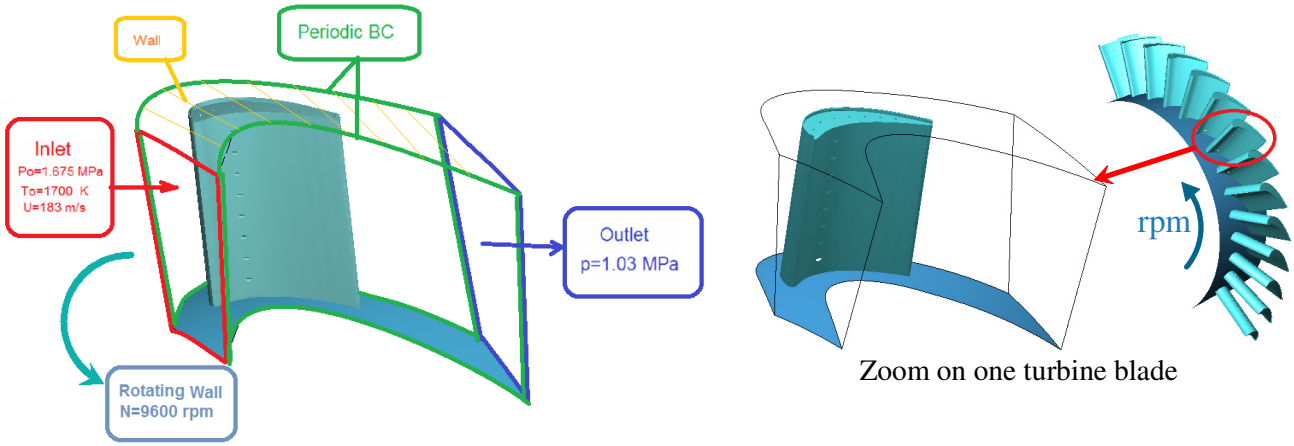

Figure 4: *Turbine blade computational domain and boundary conditions*

RESULTS

Unstructured Grid Sensitivity Analysis

A grid sensitivity analysis for a case study having a flat tip shape with tip clearance of C/H=1.5%. The results are shown in Figure 5 in terms of the average total pressure loss coefficient which is defined as follows,

$$C_{p_{av}} = \left(\frac{p_{oi} - p_{oe}}{p_{oe} - p_e} \right) \quad (1)$$

Where poi is the total relative inlet pressure, poe is the total relative exit pressure and pe is the static exit pressure.

The simulations are performed for different number of cells. The results indicate that 1.1 million cells are enough for accurate simulations.

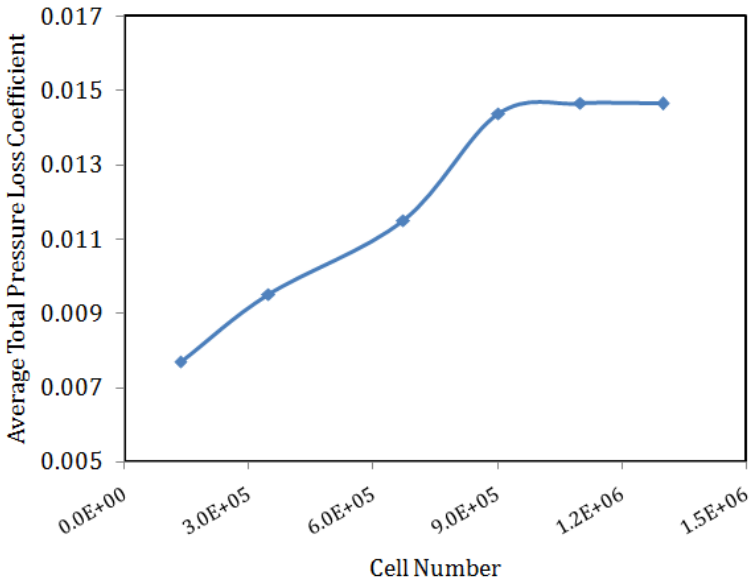

Figure 5: *Average total pressure loss coefficient versus cell number of flat tip shape with tip clearance C/H=1.5%*

Figure 6 presents the tip total pressure profile at different cutting planes along the blade chord and along the half chord thickness for different number of grid cells. The maximum total pressure drop occurs on the flat tip shape at the first third thickness of half chord. The drop in total pressure decreases with small value toward the half chord suction side which means the leakage of flow begins at half chord pressure side to suction side. The maximum total pressure obtained behind the blade leading edge and decreases toward the mid chord. For insufficient cell number, the total pressure variation from the blade tip to the case is constant or linear variation. By increasing the cell number, the total pressure profile is improved and it has the correct shape (approximately a parabolic shape). This result is obtained with control volume of 1.1 million cells.

Effect of Tip Geometry on Turbine Losses

The leakage jet essentially enters the gap isentropically up to the vena contract. Beyond this point, the manner in which the leakage flow reattaches to the tip surface behind the separation bubble and the subsequent mixing of the leakage jet and the high loss fluid from the separation bubble has been represented. The overall losses of turbine blade are due to the summation of the endwall loss, the internal gap loss and the mixing loss of leakage with the main stream flow, the last value of loss has a large contribution value of total losses. Within the bubble itself, a minimum pressure was obtained near mid chord which suggested a helical, chordwise flow of separated fluid from the leading and trailing edges towards mid chord. The accumulation of separated fluid was thought to occur at mid chord where it was forced to mix with the leakage flow as a high loss core.

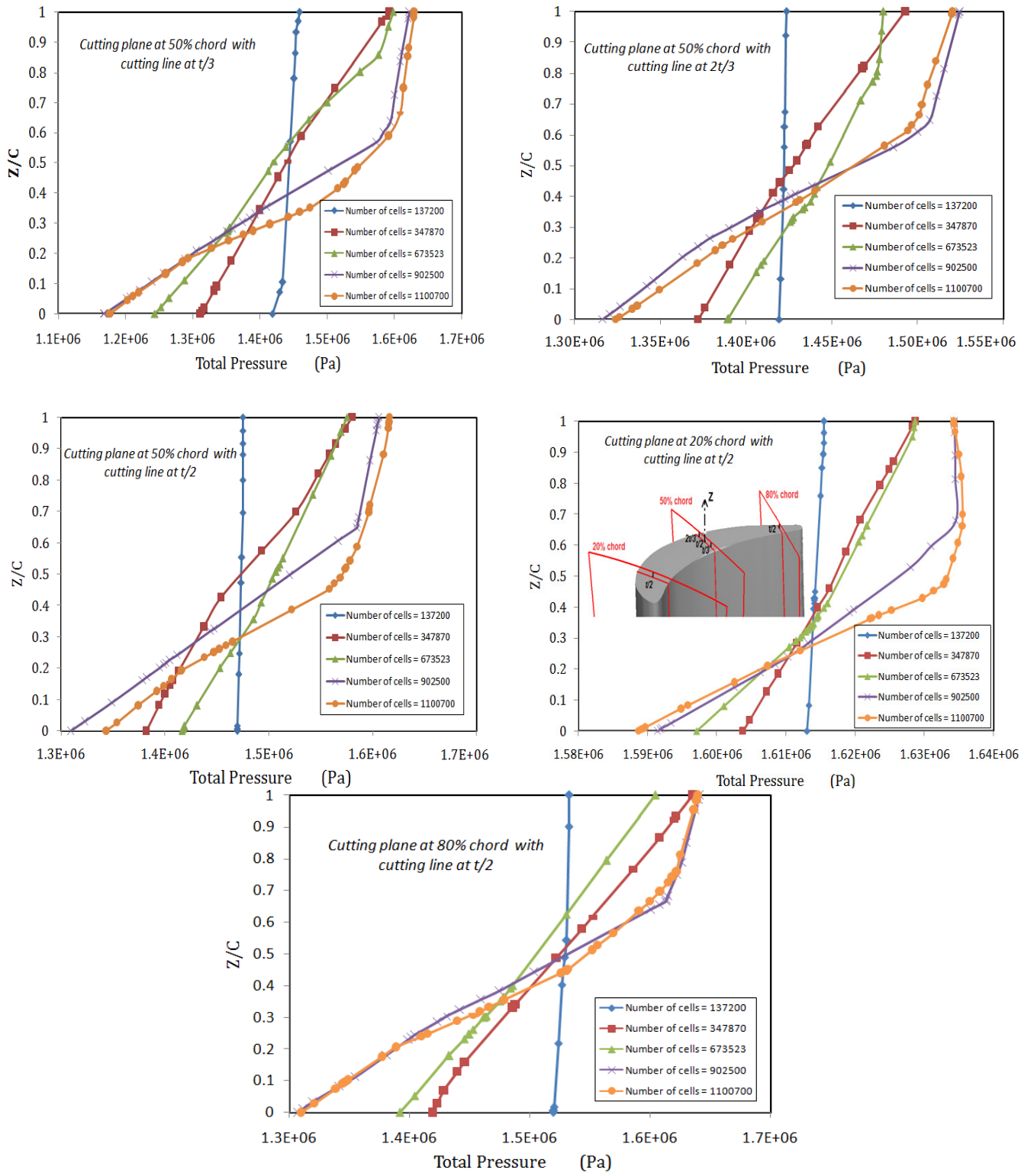

Figure 6: *Variation of a flat tip shape total pressure profile at different cutting planes along the blade chord and along the half chord thickness with tip clearance C/H=1.5%*

Figure 7 presents the pressure contour on the blade tip for different shapes. Due to the favorable pressure gradient between the pressure and suction sides of the blade, the flow is accelerated through the gap between the blade tip and the shroud. This figure indicates also that for the flat tip case the minimum pressure or separation bubble appears at the tip pressure side. This drop in the pressure increases toward the tip suction side by increasing the tip clearance. The situation is different for the case of single and double squealer tip. For a single suction side squealer tip configuration, a low value of static pressure region is also observed on top of the squealer rim. However, the high value of static

pressure (red color) is extended over the most of the blade tip cavity surface with a drastic reduction of the tip leakage flow across the suction side squealer rim. By increasing the depth of squealer cavity with different tip clearances, the pressure increases inside the squealer cavity depth which decreases the tip losses. This results can be seen clearly in case of C/H=3.5% for different cavity depths. For double squealer tip shape, by increasing the tip clearance the pressure decreases on the cavity rim depth and by increasing the depth of squealer cavity the static pressure increases similarly to single squealer tip. It is also clear from the figure that the tip configuration, which minimizes the gap losses, is the single squealer tip shape. This configuration has the maximum values of static pressure over most of the blade tip surface.

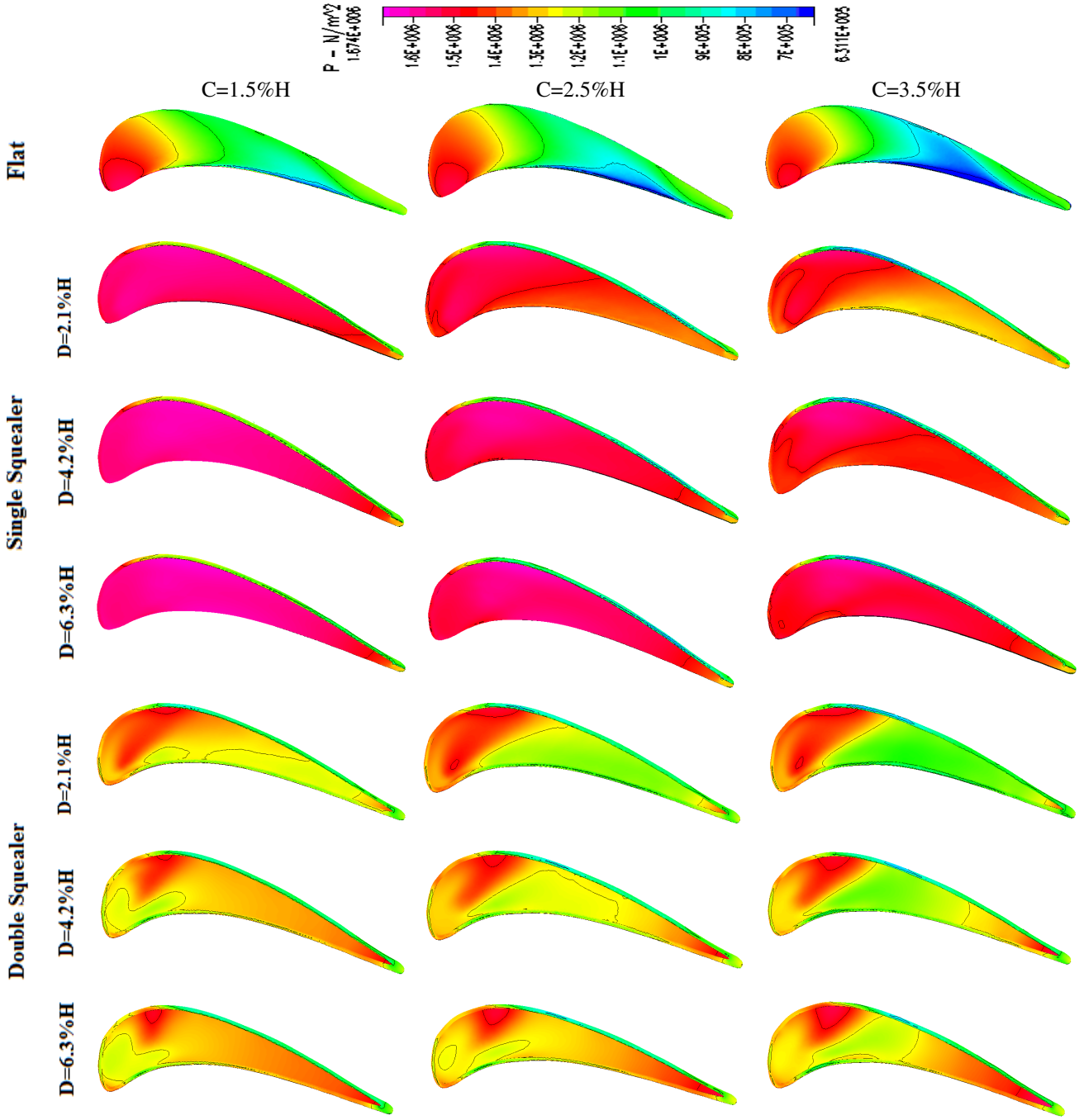

Figure 7: *Static pressure contour of different tip shapes with different tip clearances and different cavity depths*

The local total pressure loss coefficient is used in the current study to expresses the losses or the strength of the vortex inside the tip gap and the vortex of the tip leakage flow with the mainstream flow. This coefficient is defined as the difference between the inlet total pressure and the total pressure at any point divided by the exit dynamic pressure.

$$C_p = \left(\frac{p_{oi} - p_o}{p_{oe} - p_e} \right) \tag{2}$$

So, in order to show the leakage flow structure along the chord of turbine blade, which begins behind the half chord blade suction side toward the blade trailing edge, different cutting planes along the blade chord are presented at 20%, 50%, and 80% of the chord.

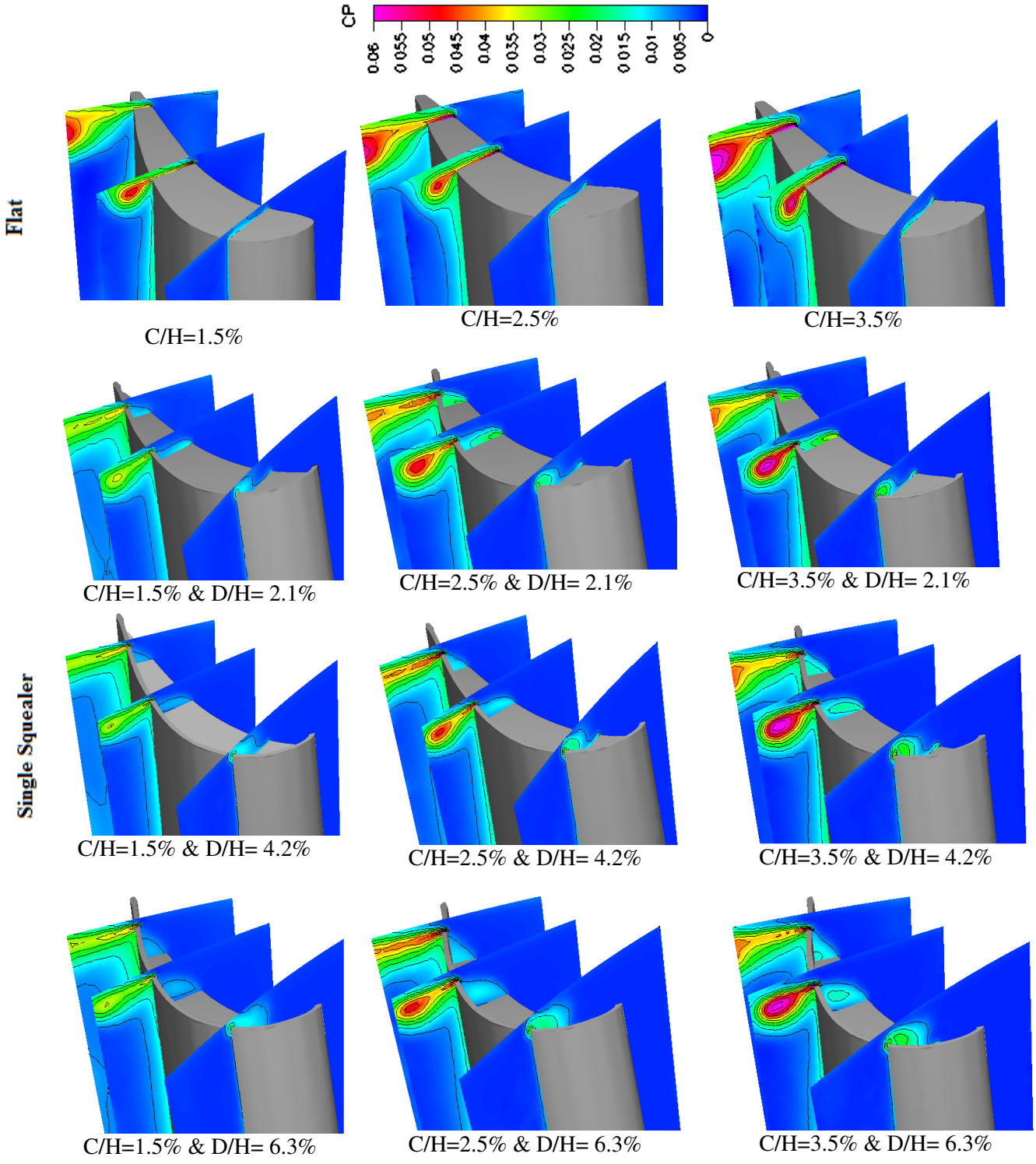

Figure 8a: *leakage flow patterns for the flat and the single squealer tip shapes with different tip clearances and tip cavity depths*

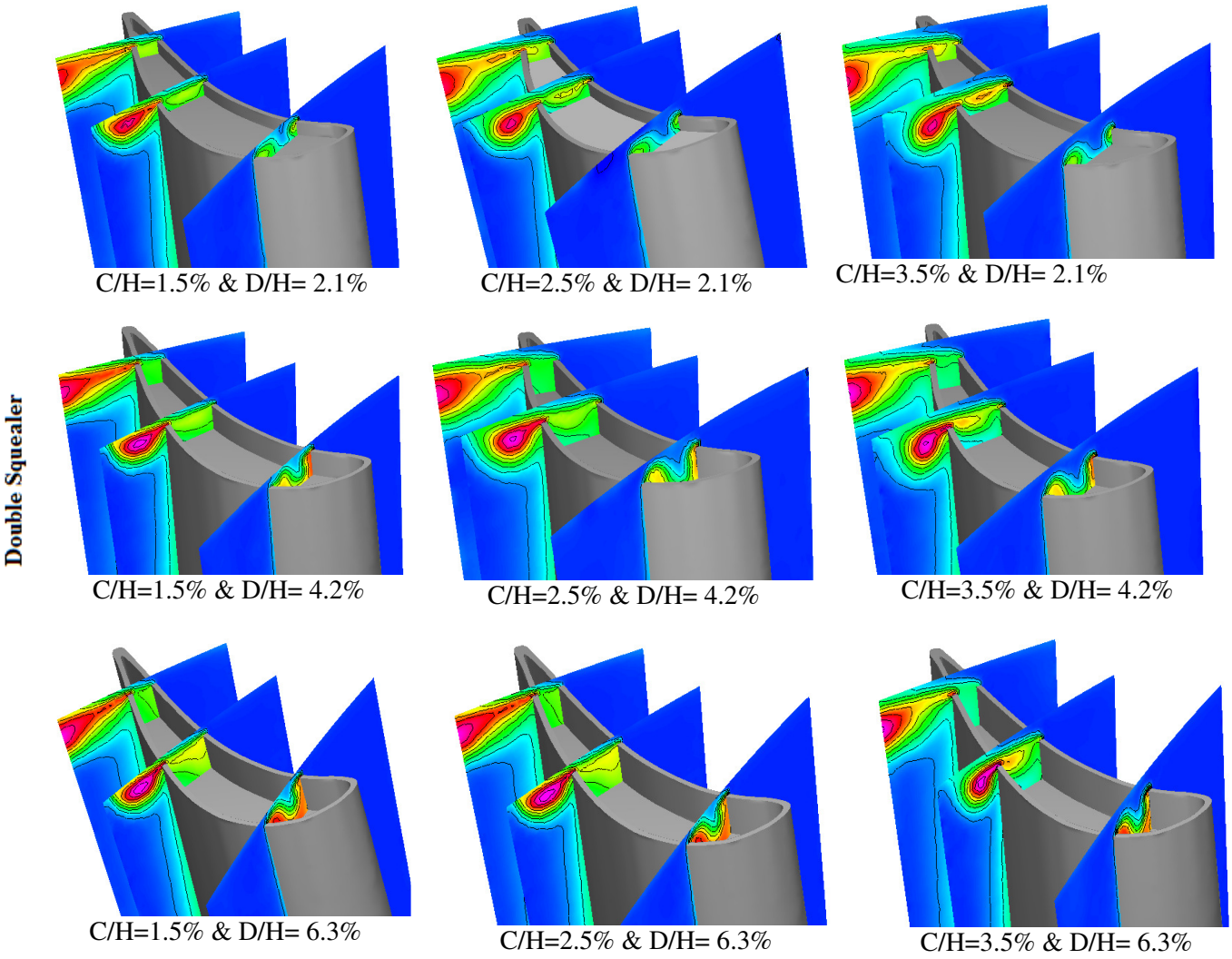

Figure 8b: *leakage flow patterns for the double squealer tip shape with different tip clearances and tip cavity depths*

Figures 8a and 8b present the local total pressure loss coefficient for different tip shapes at different cutting planes. For the flat tip shape with 20%c cutting plane, the drop in total pressure loss coefficient has a high value only at the top of the blade. At the half chord cutting plane, the total pressure loss coefficient increases at the tip gap which means a high leakage flow at this section and the begging of vortex structure formation at the blade suction side. At this section, the strength of the vortex and the mixing losses of leakage flow with the mainflow on the blade suction side increases by increasing the tip clearance. At the last cutting plane (80%c) the high vortex strengthens away from the blade suction side. The strength of this vortex increases as the tip clearance increases. This vortex structure behavior is also obtained for the single and double squealer tip shapes with different vortex strength. In addition, a new gap vortex structure is obtained due to a squealer rim.

The best tip shape in minimizing the total losses is a single squealer tip with tip clearance C/H=1.5% for different cutting planes and corresponding losses decrease by increasing the depth of squealer cavity. By increasing the tip clearance at different cutting plane the strength of vortex or leakage flow increased with small value but with corresponding jumping in gap loss. At tip clearance C/H=3.5% the gap loss and the suction side mixing losses have a maximum values. Double squealer tip shape is similar to single squealer tip in losses behavior with tip clearance and depth cavity variations. But, in a double squealer tip shape the leakage flow from pressure side circulated inside the cavity depth in direction of blade trailing edge which increasing the gap loss than the case of single squealer tip for different cutting planes at different tip clearances and cavity depths.

Figures 9a and 9b present a comparison of path lines for different tip configurations and different tip clearances. For the flat tip configuration, the fluid accelerates through the tip gap and combines with the mainstream flow away from the blade suction side to form a tip leakage vortex. The velocity of tip leakage vortex is slower than the flow in other regions.

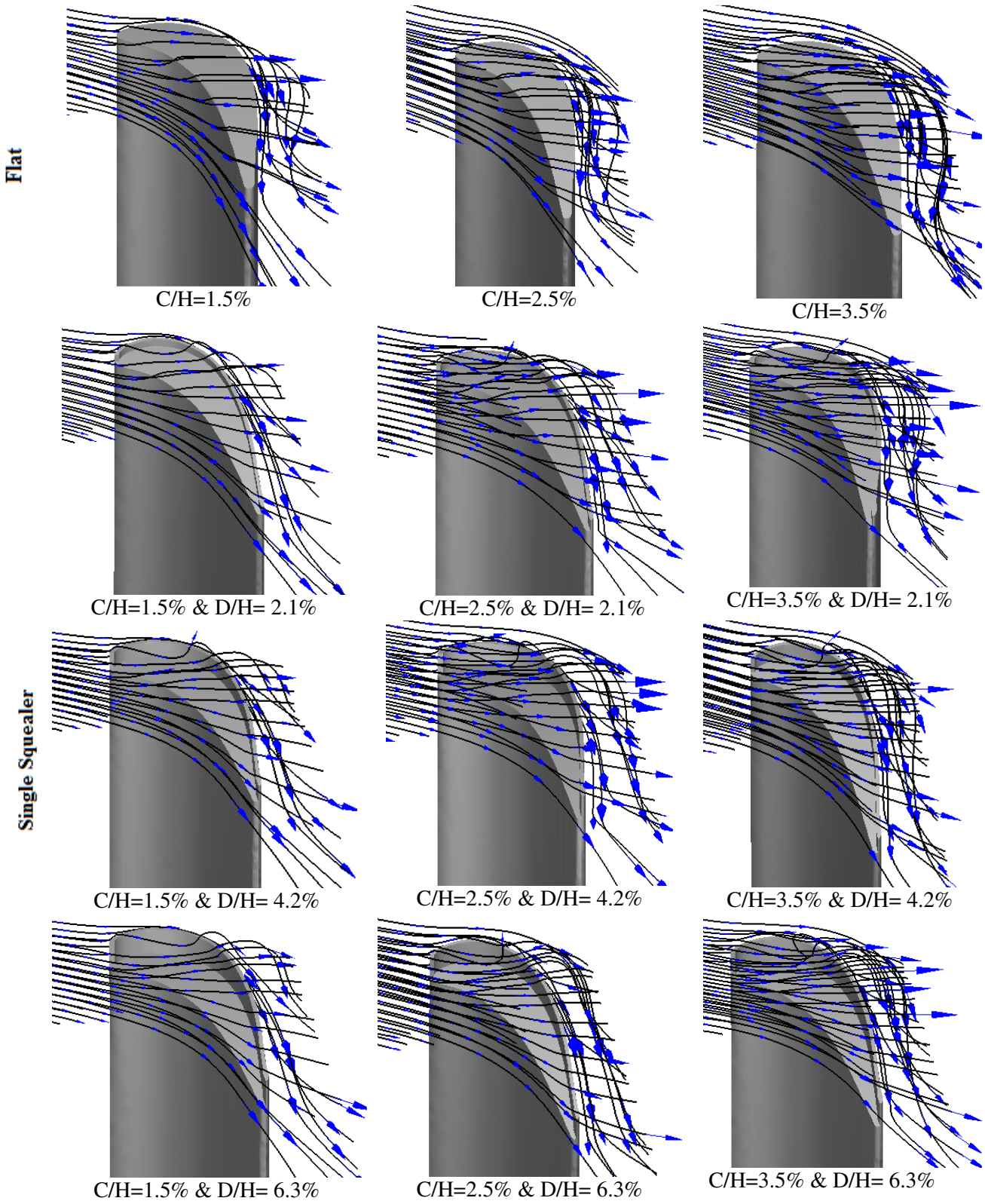

Figure 9a: *Comparison of path lines for flat tip and single suction side squealer tip configurations with different tip clearances and different squealer cavity depths*

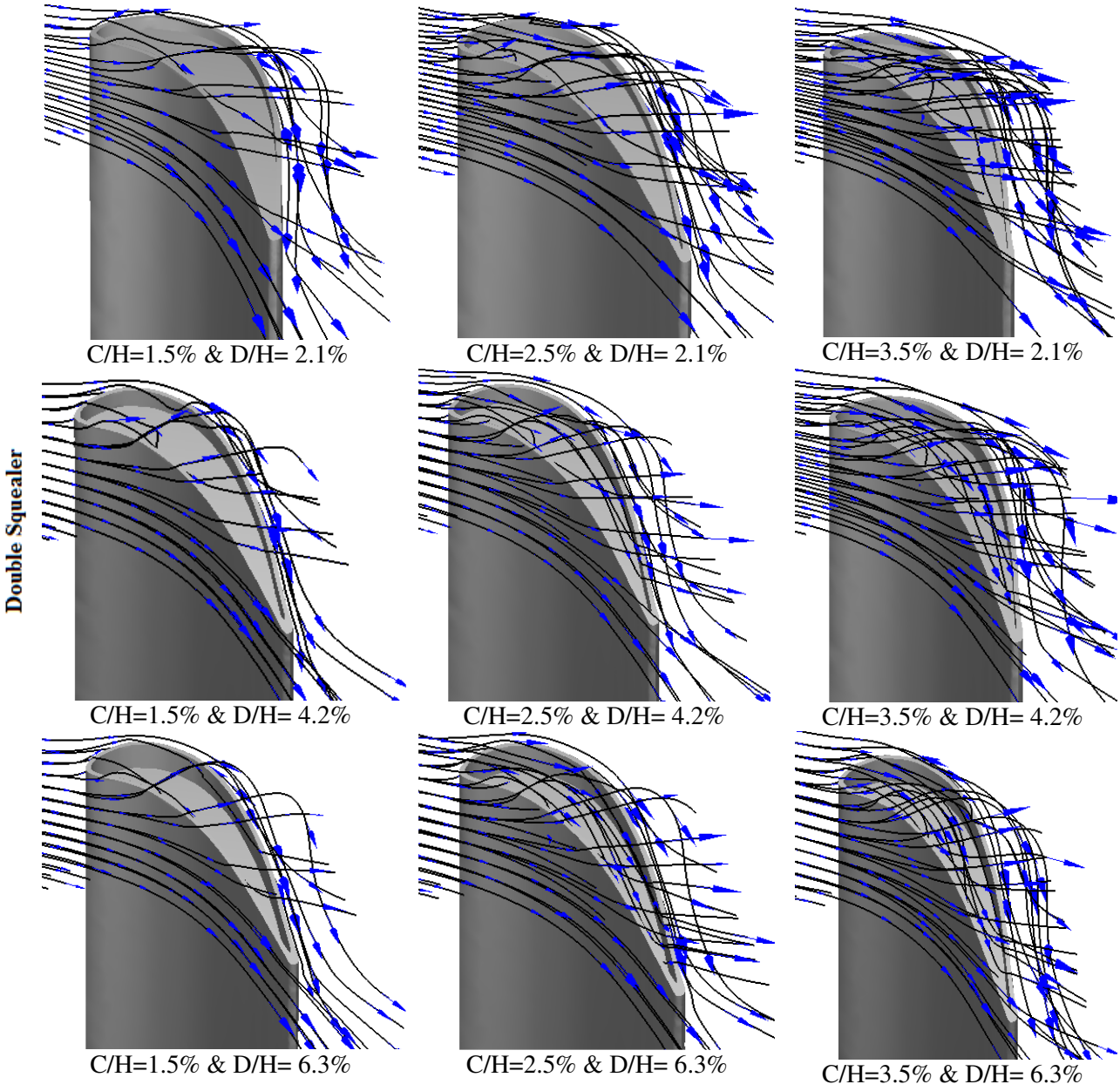

Figure 9b: *Comparison of path lines for double squealer tip configuration with different tip clearances and different squealer cavity depths*

For the single suction side squealer tip configuration, a leakage vortex is formed along the junction of the blade tip and the squealer rim as clear from figure 9a. The vortex rolls up across the squealer rim and merges into the tip leakage vortex near the blade suction side. For the double squealer tip, the flow structure around the tip is more complicated than the other two cases. A tip leakage vortex is formed near the blade suction side and another vortex is formed inside the squealer cavity when the fluid enters the squealer cavity from the leading edge and pressure side of the blade tip. The vortex rolls down the pressure side squealer rim to form a large recirculation flow region inside the squealer cavity. It then rolls up across the suction side squealer rim and merges into the suction side tip leakage vortex. Also it is found that the velocity of vortex inside the squealer cavity decreases from the leading edge to the trailing edge. In addition, the number of path lines increases by increasing the tip clearance for the different tip shapes. Thus, the tip losses increase by increasing the tip clearance. The roll of path lines inside the squealer cavity becomes clear as the depth of squealer cavity increases.

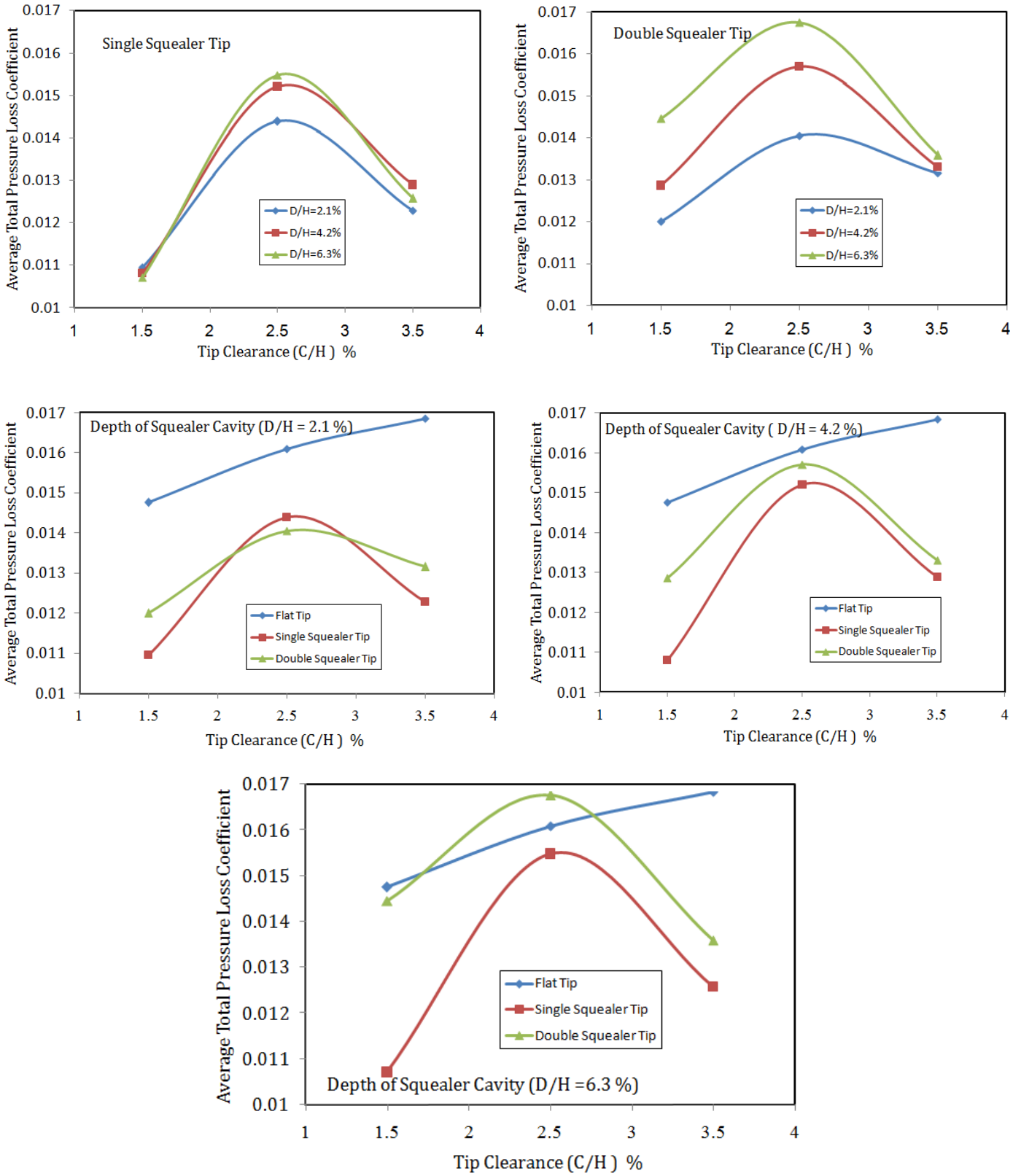

Figure 10: *Variation of average total pressure loss coefficient of different turbine tip shapes with different tip clearances and different cavity depths*

Figure 10 presents the variation of average total pressure loss coefficient for different tip shapes and different tip clearances. It is clear from the figure that minimum pressure losses are obtained for the single squealer tip shape. However, at a tip clearance of 2.5% and a cavity depth of 2.1%, the double squealer tip has a lower value of the pressure loss since the single squealer tip has a high gap loss value at this case compared to the other cases as indicated in Figures 8a and 8b. But at a high

value of squealer cavity depth (D/H= 6.3%) the flat tip shape is better than double squealer tip for a tip clearance of 2.5% since the double squealer tip at this case has a high gap loss compared to flat tip shape especially at 20%c cutting plane. The flat tip shape produces large pressure losses since this shape does not accelerate the local flow in the narrow gap on the top of the squealer rim. Thus the leakage is increased for this tip shape. The pressure loss for the double squealer shape increases with increasing the squealer cavity depth as a result of the gap loss increase.

Effect of Tip Geometry on Turbine Tip Film Cooling Effectiveness

Effect of tip hole positions: The leakage flow has a great effect in guiding the cooling flow of different tip shapes. In case of flat tip shape the leakage flow from pressure side to tip suction side, so the best hole position in good cooling of turbine tip blade with a hole array located at $L/t = 0.2$. Figure 11 indicates that increasing the blowing ratio improves the tip film cooling effectiveness. The blowing ratio and the film cooling effectiveness are defined as follows,

$$M = \left(\frac{\rho_c v_c}{\rho_h v_h} \right) \tag{3}$$

$$\eta = \left(\frac{T_{oi} - T}{T_{oi} - T_c} \right) \tag{4}$$

The lift off phenomena does not appear although the streamwise angle has a high value of 90 degrees. Low values of tip clearances prevent the lift-off and produces good tip cooling.

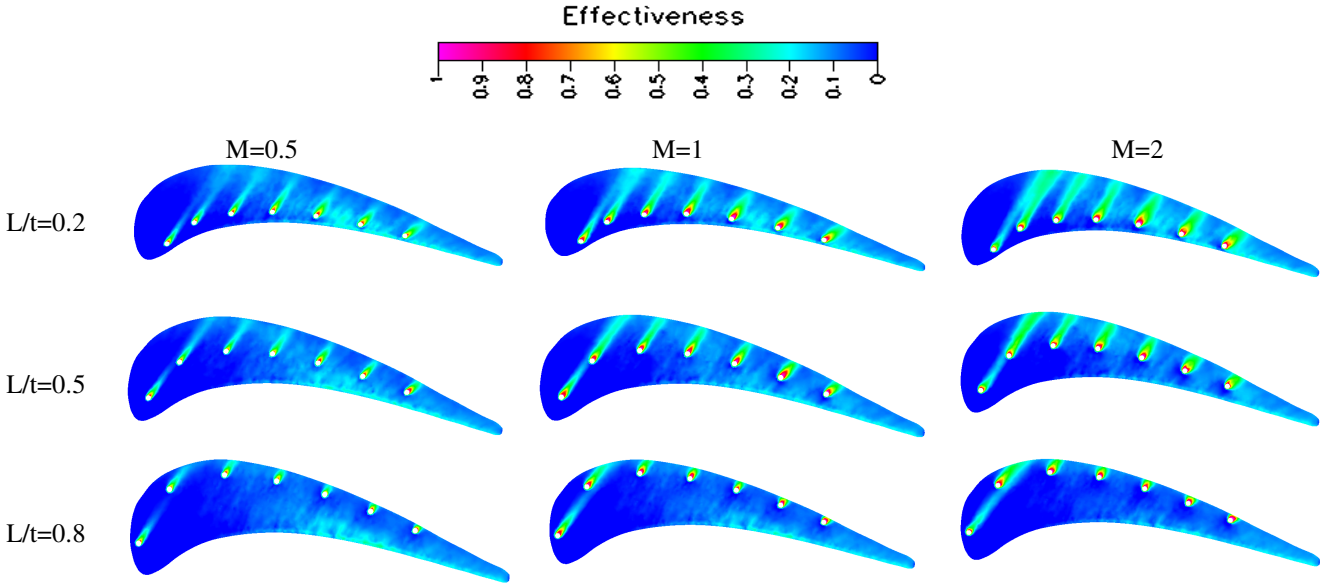

Figure 11: *Flat tip effectiveness contours with tip clearance C/H=1.5% for different holes positions and different blowing ratios*

Figure 12 presents a single squealer tip shape film cooling with different holes positions. The leakage flow corresponding to this shape is in the direction of squealer rim suction side so the best hole positions is fore a hole array located at $L/t = 0.2$ which is similar to the flat tip shape. But, the cooling process is better than flat tip cooling as the cooling flow does not leakage to the tip suction side until it cools the most tip squealer cavity area before leakage. It is clear from the figure that, the film cooling effectiveness increases by increasing of blowing ratio up to M=1, lift-off phenomenon appears clearly at blowing ratio M=2 since high gap between the blade tip and casing (summation of tip clearance and cavity depth) which minimizes the tip cooling.

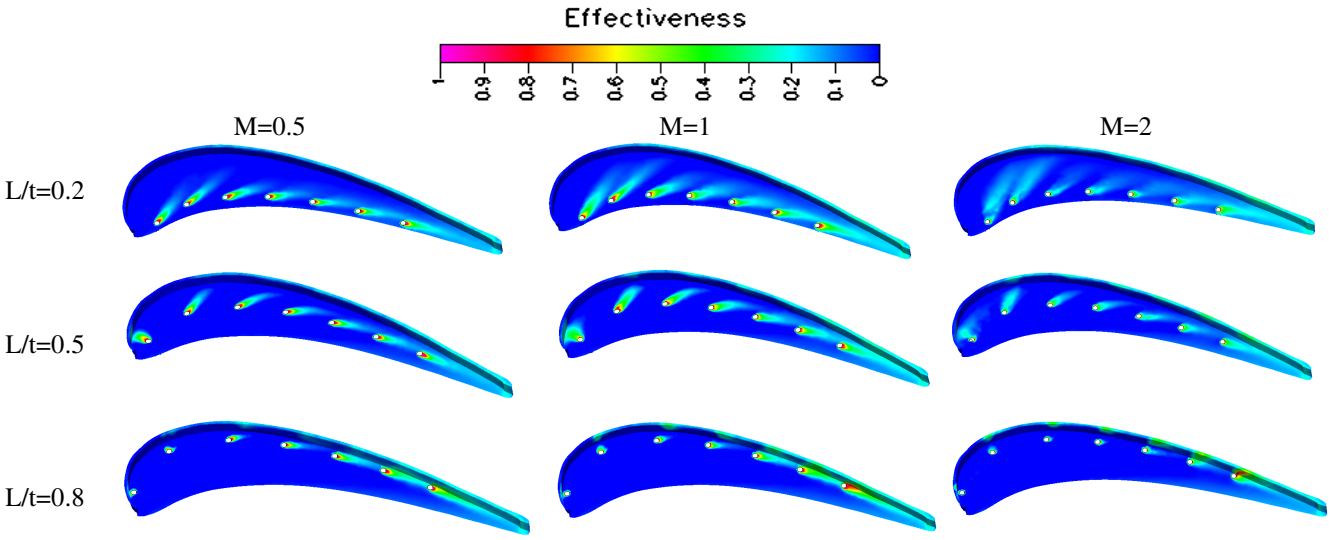

Figure 12: *Single squealer tip effectiveness contours with tip clearance C/H=1.5% and depth of squealer cavity D/H=2.1% for different holes positions and different blowing ratios*

Figure 13 presents a double squealer tip shape film cooling with different hole positions, the leakage flow accelerates in the narrow gap on the top of the squealer rim or in trailing edge direction which guides the cooling flow in direction of trailing edge pressure side, so the best hole position for this shape at tip camber line followed by hole position located at $L/t = 0.8$ and the worst position located at $L/t = 0.2$. At the worst position the cooling holes cool only the pressure side squealer rim and the rest of squealer tip cavity area without cooling. In additions, the film cooling effectiveness increases by increasing the blowing ratio.

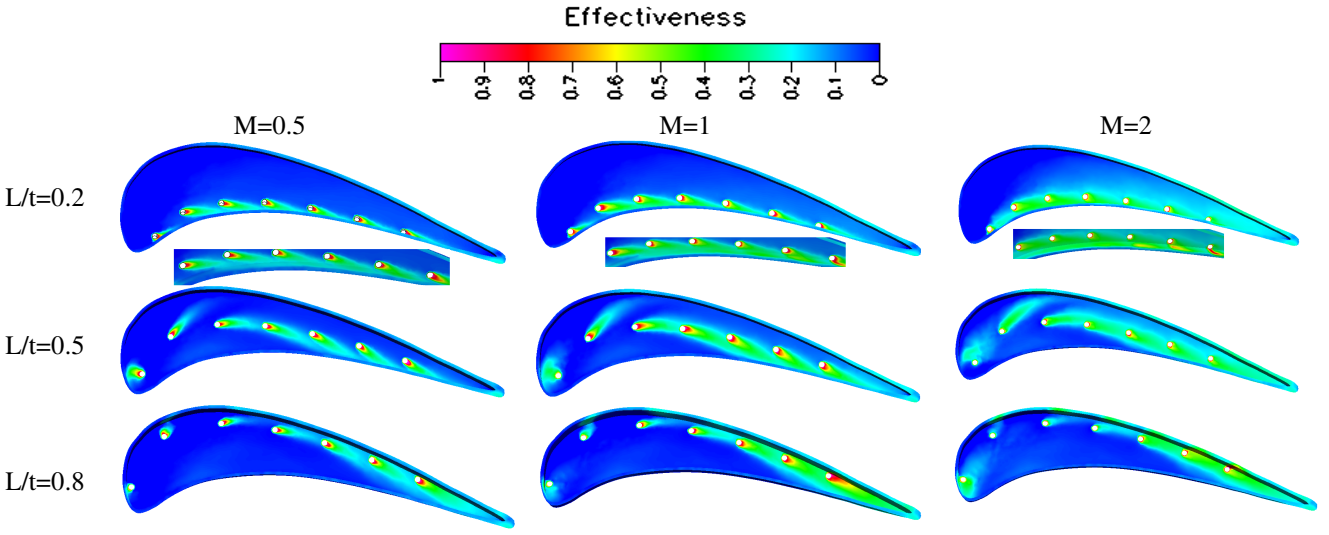

Figure 13: *Double squealer tip effectiveness contours with tip clearance C/H=1.5% and depth of squealer cavity D/H=2.1% for different holes positions and different blowing ratios*

Figure 14 presents the behavior of average overall film cooling effectiveness versus the blowing ratio for different holes positions with different tip shapes. The best hole position for a flat and single squealer tip shape to obtain the maximum average overall film cooling effectiveness located at $L/t = 0.2$ for different blowing ratios followed by camber line hole position and the worst position of film cooling holes located at $L/t = 0.8$. The optimum film cooling effectiveness of single squealer tip shape with blowing ratio M=1 but for a flat tip shape the average overall film cooling effectiveness increased or remains constant by increasing the blowing ratio from M=1 to M=2. The best hole position for a double squealer tip shape to obtain the maximum average overall film cooling effectiveness located at the tip camber line for a different values of blowing ratios at this position the

cooling flow guiding by vortex rolls down the pressure side squealer rim to obtain a good cooling inside the region of squealer rim cavity area.

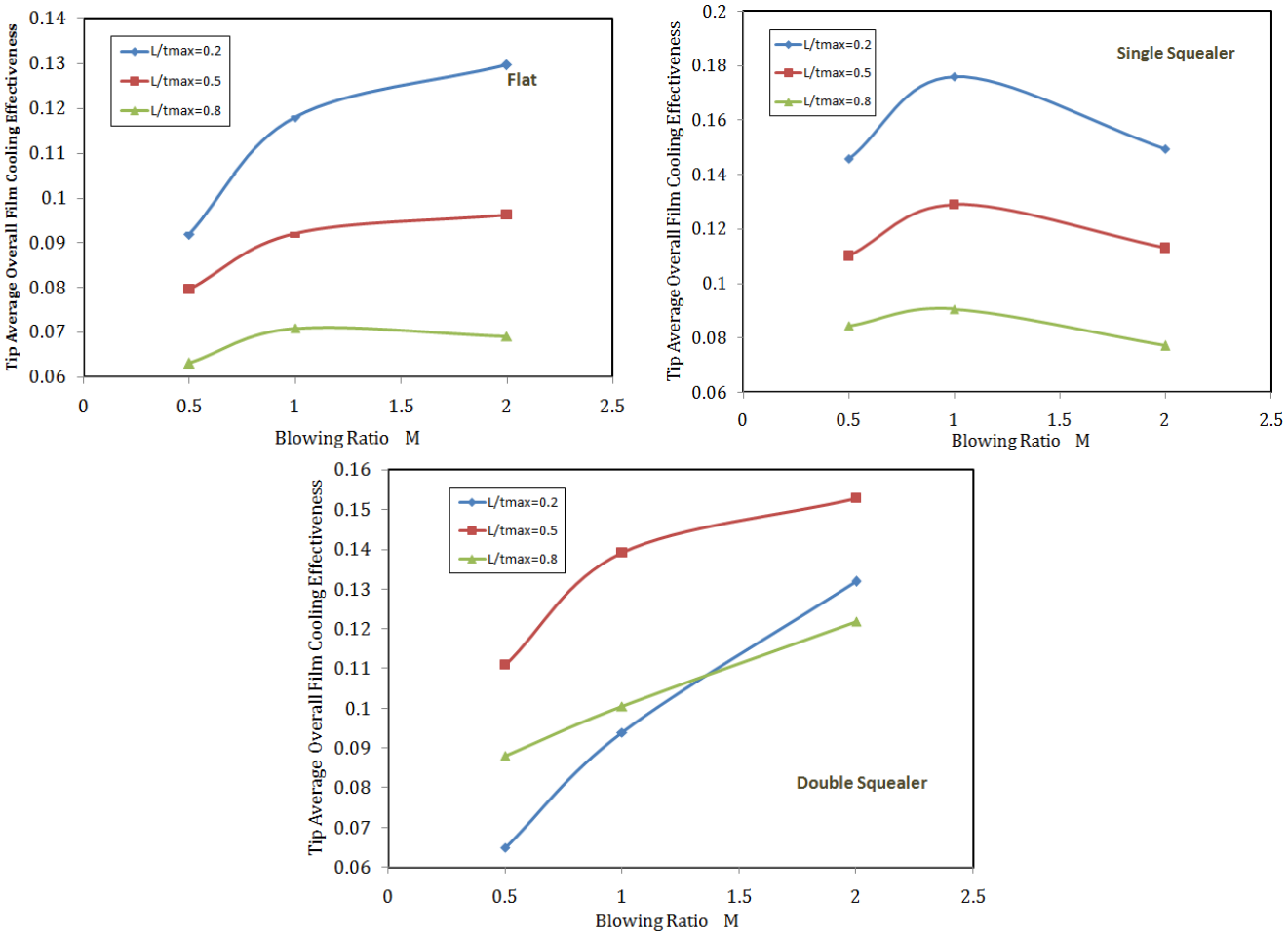

Figure 14: *Tip average overall film cooling effectiveness versus blowing ratio for different tip shapes with tip clearance C/H=1.5%, depth of squealer cavity D/H=2.1% and different holes positions*

The difference between Figure 14 and 15 that Figure 15 presents the variation of average overall film cooling effectiveness with blowing ratio for different tip shapes with different hole positions. This figure shows that, at a hole position located at $L/t = 0.2$ the single squealer tip is the best tip shape with this cooling hole position in maximizing the average overall film cooling effectiveness for a different values of blowing ratio then the flat tip shape followed by double squealer tip shape. But, the maximum average overall film cooling effectiveness with holes position located at $L/t = 0.5$ and $L/t = 0.8$ is for a double squealer tip shape with different blowing ratios followed by single squealer tip and the worst shape is a flat tip shape at these positions.

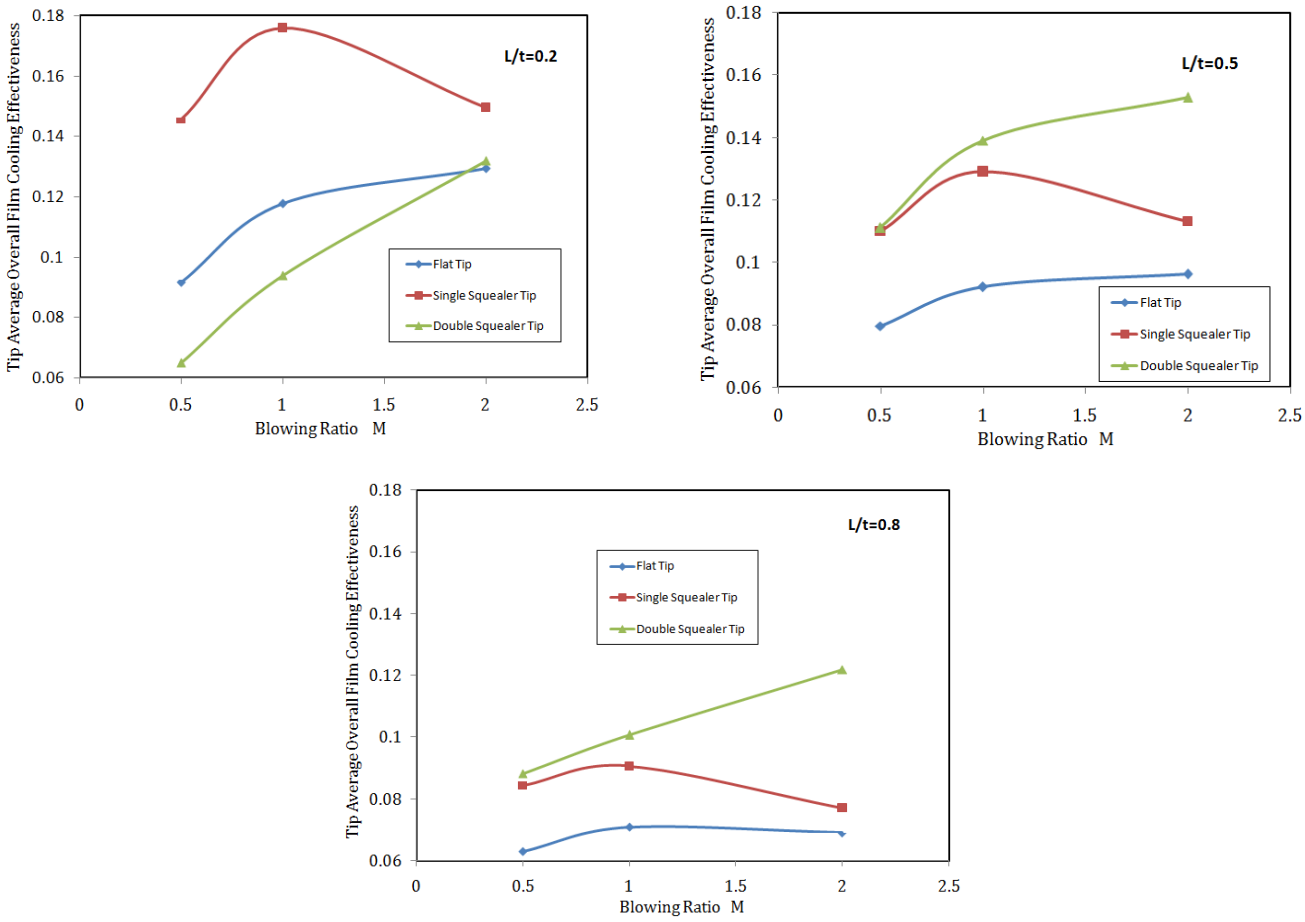

Figure 15: *Tip average overall film cooling effectiveness versus blowing ratio for different holes positions with different tip shapes of tip clearance C/H=1.5% and depth of squealer cavity D/H=2.1%*

Figure 16 presents Path lines contours colored by static temperature of different tip configurations for a seven camber line holes with C/H=1.5%, D/H=2.1% and blowing ratio M=1. It is clear from the figure that, the leakage flows guiding the cooling flow of different tip shapes. In case of flat tip shape the leakage flow direct the cooling flow from pressure side to tip suction side, so the tip surface has a low cooling. But, the existence of single suction side squealer rim guides the leakage and cooling flows within it in trailing edge direction which improves the cooling tip squealer cavity than flat tip shape. The double squealer tip shape directs the leakage flow with cooling in the narrow gap on the top of the squealer cavity or in trailing edge pressure side direction. At this tip shape the cooling flow covers the most surface of top squealer cavity area.

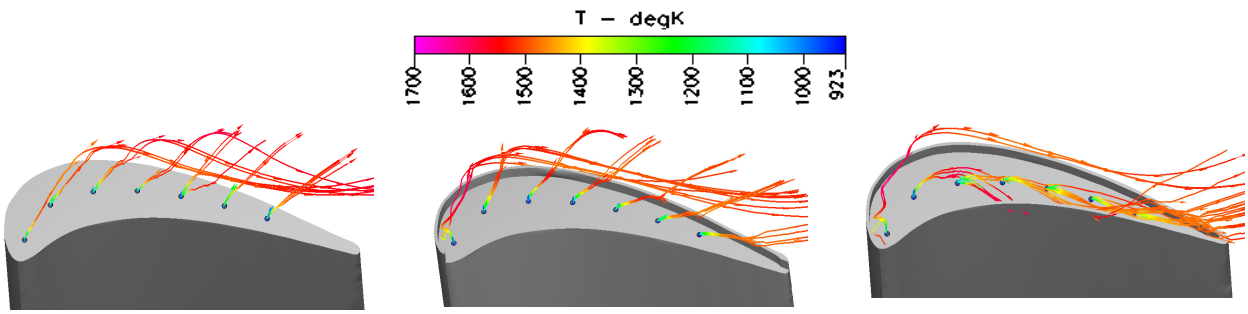

Figure 16: *Path lines (colored by static temperature) of different tip configurations for seven camber line holes with C/H=1.5%, D/H=2.1% and blowing ratio M=1*

Effect of Streamwise Angle for Single Squealer Tip shape with Tip Clearance C/H=1.5%, Depth of Squealer Cavity D/H= 2.1%, and Blowing Ratio M=1: The streamwise angle has a significant effect in the film cooling effectiveness as shown in Figure 17. This figure shows the contours of film cooling effectiveness of camber line CYSA film cooling holes on single squealer tip shape with tip clearance C/H=1.5%, depth of squealer cavity D/H= 2.1%, and blowing ratio M=1. The figure indicate that, the film cooling effectiveness increases by decreasing the streamwise angle and the maximum film cooling effectiveness is obtained at a streamwise angle of 30 degree. At streamwise angle of 90 degree, the counter rotating vortex pair of the mixing between the mainstream and cooling flows is strong enough such that the cooling flow experiences the lift-off phenomenon. Thus, the cooling effectiveness is reduced at this streamwise angle. The strength of vortex pair increases by increasing the value of blowing ratio. On the opposite, for streamwise angle of 30 degree the cooling flow is attached to the tip surface without lift off and good cooling is obtained.

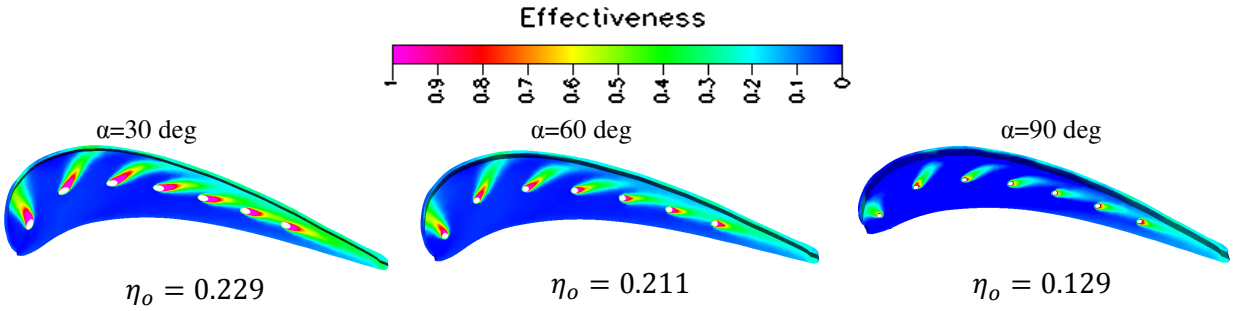

Figure 17: *Single squealer tip effectiveness contours for seven camber line holes with tip clearance C/H=1.5%, depth of squealer cavity D/H=2.1%, M=1 and different streamwise angles*

Effect of Tip Clearance of Flat Tip shape with Streamwise Angle 90 deg and Blowing Ratio M=1: Figure 18 presents the contours of film cooling effectiveness of camber line CYSA film cooling holes on a flat tip shape with different tip clearance and blowing ratio M=1. The tip clearance has insignificant effect on the film cooling effectiveness compared to streamwise angle and blowing ratio effect. The results also indicate that the film cooling effectiveness decreases slowly by increasing tip clearance due to the effect of the lift-off phenomenon.

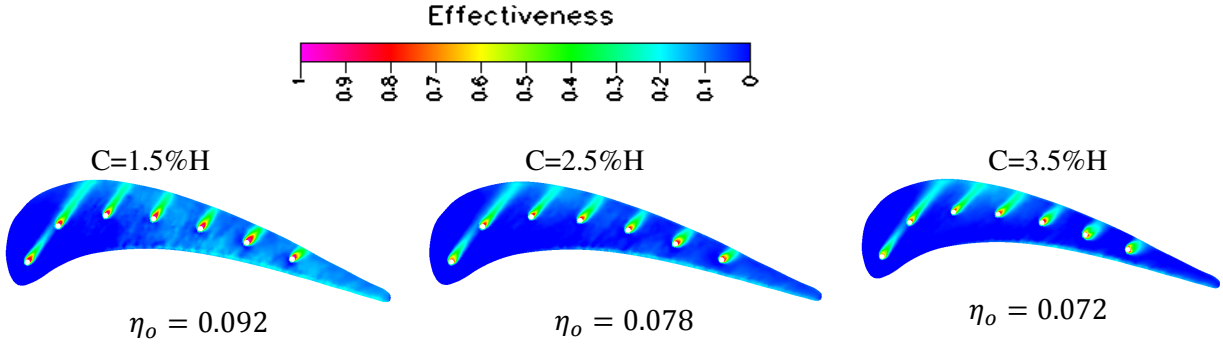

Figure 18: *Flat tip effectiveness contours for seven camber line holes with blowing ratio M=1 and different tip clearances*

Effect of Tip Film Cooling of Different Tip shapes with Streamwise Angle 90 deg, Blowing Ratio M=1and Camber Line Holes Position on Turbine Losses

The film cooling holes have a significant effect on the tip losses. The blade tip film cooling reduces the tip leakage mass flow rate for both the flat and squealer tip configurations. Figure 19 presents a comparison of average total pressure loss coefficient variation versus tip clearance of various tip shapes with and without film cooling. The results indicate that the different tip shapes with film cooling reduces the tip pressure losses. The drop in the average total pressure loss coefficient decreases as the tip clearance increases up to a tip clearance of 3.5%. The results also show that the single squealer cavity with film cooling has the minimum pressure losses.

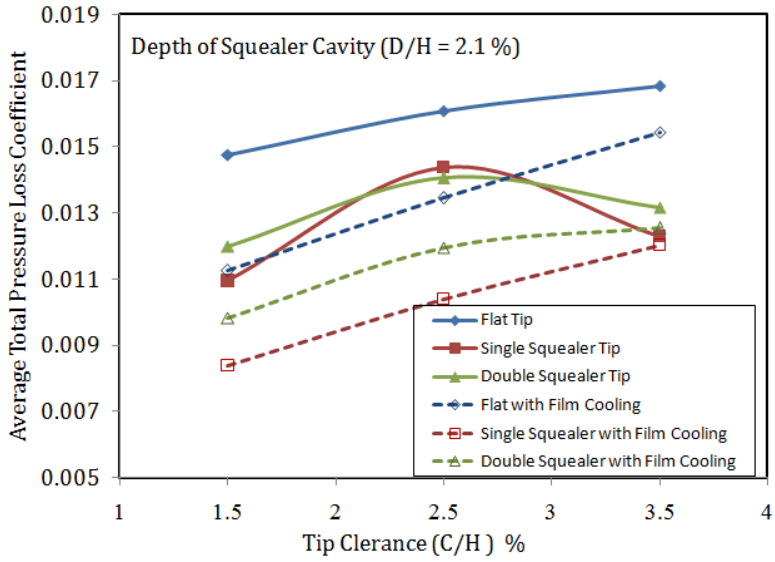

Figure 19: *Comparison of average total pressure loss coefficient versus tip clearance of various tip shapes with and without film cooling and the depth of squealer cavity D/H= 2.1%*

CONCLUSIONS

The numerical simulation of the flow through turbine blade and the coolant flow through blade with tip-hole system is carried out using the "CFDRC package". Unstructured finite volume technique is used to solve the steady, three-dimensional and compressible Navier-Stokes equations. A parametric study is performed for the flat and squealer tip shape with film cooling hole to determine the optimum tip shape that could minimize the total pressure loss coefficient and maximize the tip cooling effectiveness. The effect of film cooling parameters such as the position of the film-cooling hole, the streamwise angle and the blowing ratio on the cooling effectiveness is studied. Optimum cooling parameters are selected for different tip configurations. The results indicate that the squealer tip has a great effect in minimizing the turbine loss and hence the cooling requirements. However, the single squealer tip shape has minimum total pressure losses for different tip clearance and different cavity depth except at C/H=2.5% & D/H= 2.1%. In addition, the single squealer tip has maximum average overall film cooling effectiveness for film cooling holes located on tip pressure side ($L/t = 0.2$). The tip average overall film cooling effectiveness increases by increasing the value of blowing ratio up to M=1 for different tip shapes. The optimum streamwise angle which maximizes the overall film cooling effectiveness is 30 deg. The film cooling effectiveness increases with a small value by decreasing the tip clearance. The blade tip film cooling not only increases the cooling effectiveness but also reduces the tip leakage mass flow rate for both the plane and squealer tip configurations.

NOMENCLATURE

C Blade Tip Clearance, [m] or Blade Chord, [m]

C_p Local Total Pressure Loss Coefficient, $\left(\frac{p_{oi} - p_o}{p_{oe} - p_e}\right)$

$C_{p_{av}}$ Average Total Pressure Loss Coefficient, $\left(\frac{p_{oi} - p_{oe}}{p_{oe} - p_e}\right)$

D Hole Diameter, [m] or Squealer Cavity Depth, [m]

H Blade Height, [m]

L The Hole Position Located on Blade Tip Measured from Pressure to Suction Side, [m]

M Blowing Ratio, $\left(\rho_c v_c / \rho_h v_h\right)$

p_i Static Pressure Inlet, [Pascal]

p_o Local Total Pressure , [Pascal]

p_{oe} Total Pressure Outlet, [Pascal]

p_{oi} Total Pressure Inlet, [Pascal]

t Blade Tip Thickness, [m]

T Wall Temperature at any Point, [K]

T_{av} Average Wall Temperature, [K]

T_c Temperature of Coolant Air, [K]

T_{oi} Turbine Total Inlet Temperature, [K]

v_c Velocity of Coolant Air, [m/s]

v_h Velocity of Hot Gases, [m/s]

GREEK SYMBOLS

α Streamwise (simple) Angle

η Film Cooling Adiabatic Effectiveness, $\left(\frac{T_{oi}-T}{T_{oi}-T_c}\right)$

η_o Average Overall Film Cooling Adiabatic Effectiveness, $\left(\frac{T_{oi}-T_{av}}{T_{oi}-T_c}\right)$

ρ_c Density of Coolant Air, [Kg/m^3]

ρ_h Density of Hot Air, [Kg/m^3]

References

Azad, Gm. S., Han, J.C., Boyle, R.J. (2000) Heat Transfer and Flow on the Squealer Tip of a Gas Turbine Blade, ASME paper 2000-GT-195, 2000.

Heyes, F.J.G. and Hodson, H.P., Dailey, G.M (1992) The Effect of Blade Tip Geometry on the Tip Leakage Flow in Axial Turbine Cascades, ASME Journal of Turbomachinery, Vol.114, pp.643-651, 1992.

Bunker, R.S. and Bailey, J.C. (2000) Blade Tip Heat Transfer and Flow with Chordwise Sealing Strips, International Symposium on Transport Phenomena and Dynamics of Rotating Machinery (ISROMAC), Honolulu, Hawaii, pp.548-555, 2000.

Ameri, A.A. (2001) Heat Transfer and Flow on the Blade Tip of a Gas Turbine Equipped with a Mean Camber-line Strip, ASME Journal of Turbomachinery, Vol.123, pp.704-708, 2001.

Ameri, A.A., Steinthorsson, E., Rigby, L.D. (1997) Effects of Squealer Tip on Rotor Heat Transfer and Efficiency, ASME paper 1997-GT-128.

Azad, Gm. S., Han, J.C., Bunker, R.S.,Lee,C.P. (2001) Effect of Squealer Geometry Arrangement on Gas Turbine Blade Tip Heat Transfer, ASME/IMECE 2001/HTD-24314, HTD-Vol.369-5, pp.297-305, 2001.

Ameri, A.A. and Bunker, R.S. (2000) Heat Transfer and Flow on the First Stage Blade Tip of a Power Generation Gas Turbine: Part 2: Simulation Results, ASME Journal of Turbomachinery, 122, No. 2, pp. 272-277, 2000.

Bunker, R. S., Baily, J.C., and Ameri, A.A. (2000) Heat Transfer and Flow on the First Stage Blade Tip of a Power Generation Gas Turbine: Part 1: Experimental Results, ASME Journal of Turbomachinery, 122, No.2, pp. 263-271, 2000.

Ameri, A.A. (2001) Heat Transfer and Flow on the Blade Tip of a Gas Turbine Equipped With a Mean-Camberline Strip, ASME Journal of Turbomachinery, 123, No.4, pp. 704-708, 2001.

Yang, H., Acharya, S., Ekkad, S. V., Prakash, C., and Bunker, R (2002) Flow and Heat Transfer Predictions for A Flat-Tip Turbine Blade, Proceedings of ASME Turbo Expo, ASME Paper GT-2002-30190, 2002.

Yang, H., Acharya, S., Ekkad, S.V., Prakash, C., and Bunker, R. (2002) Numerical Simulation of Flow and Heat Transfer Past a Turbine Blade with a Squealer-Tip, Proceedings of ASME Turbo Expo, ASME Paper GT-2002-30193.

Azad, GM S., Han, J.C., Teng, S., and Boyle, R. (2000) Heat Transfer and Pressure Distributions on a Gas Turbine Blade Tip, ASME Journal of Turbomachinery, 122, No.4, pp.717-724, 2000.

Azad, GM S., Han, J.C., and Boyle, R. (2000) Heat Transfer and Pressure Distributions on the Squealer Tip of a Gas Turbine Blade, ASME Journal of Turbomachinery, 122, No.4, pp. 725-732, 2000.

Kwak, J.S., and Han, J.C. (2003a) Heat Transfer Coefficients and Film-Cooling Effectiveness on a Gas Turbine Blade Tip, Journal of Heat Transfer, 125(3), 494–502, DOI: 10.1115/1.1565096, 2003.

Kwak, J., and Han, J.C. (2003b) Heat transfer coefficients and film cooling effectiveness on the squealer tip of a gas turbine blade, Journal of Turbomachinery, 125, 648, 2003.

Christophel, J.R., Thole, K.A., and Cunha, F.J. (2005) Cooling the Tip of a Turbine Blade Using Pressure Side Holes—Part I: Adiabatic Effectiveness Measurements, Journal of Turbomachinery, 127(2), 270–277, DOI: 10.1115/1.1812320, 2005.

Ahn, J., Mhetras, S., and Han, J.C. (2005) Film-Cooling Effectiveness on a Gas Turbine Blade Tip Using Pressure-Sensitive Paint, Journal of Heat Transfer, 127, 521–530, DOI: 10.1115/1.1909208, 2005.

Mhetras, S., Narzary, D., Gao, Z., and Han, J.C. (2008a) Effect of a Cutback Squealer and Cavity Depth on Film-Cooling Effectiveness on a Gas Turbine Blade Tip, Journal of Turbomachinery, 130, 021002, DOI: 10.1115/1.2776949, 2008.

Gao, Z., Narzary, D., Mhetras, S., and Han, J.C. (2009b) Effect of Inlet Flow Angle on Gas Turbine Blade Tip Film Cooling, Journal of Turbomachinery, 131, 031005, DOI: 10.1115/1.2987235, 2009.

Rallabandi, A.P., Grizzle, J., and Han, J.C. (2008) Effect of upstream step on flat plate film cooling effectiveness using PSP, Proceedings of the ASME Summer Heat Transfer Conference, HT08-56194, vol. 2, 599 – 609, Jacksonville, FL, United states, 2008.